

## LUNG FIELD SEGMENTATION ON COMPUTED TOMOGRAPHY IMAGE USING REGISTRATION

Oleh :

**SRI WIDODO**

APIKES Citra Medika Surakarta

E-mail: papa\_lucky01@yahoo.com

### ABSTRACT

*During recent years, research on lung nodules detection is still much discussed by the researchers. Automatic lung nodule detection generally consists of two steps, namely lung nodule candidate detection and classification to determine nodule. Detection of nodule candidates begins with segmenting lung field. Current method is widely used for lung field segmentation of CT scan image is Thresholding and Active Contour, which relies on contrast of gray values between lung parenchyma and surrounding tissues. Drawback of both methods is that if nodule is large and located on borders of lung, then nodules will not be included in the image of lung (nodules contained will be lost). This means that segmentation of lung field was considered a failure, because image of nodule is object of attention will be lost.*

*Purpose of this research is lung field segmentation that contain abnormalities in CT scan image using registration methods. Registration is used namely elastic registration (non-rigid registration). We also perform lung fields segmentation using thresholding and Active Contour, as a comparison with method we proposed. Results of our study show that segmentation with registration approach has accuracy 95.5%, sensitivity 91.5%, and specificity of 96.6%. Segmentation with threshold has accuracy 92.2%, sensitivity 91.3%, and specificity 92.4%. While segmentation with Active Contour has accuracy 92.4%, sensitivity 87.5%, and specificity of 93.7%.*

**Keywords: active contour, non-rigid registration, lung field, thresholding.**

### INTRODUCTION

Lung nodules are one type of abnormality in lung organ can also be possibility of lung cancer. While lung cancer is all of malignancies disease in lung. Malignancy can be derived from lung itself (primary) or spread (metastasis) of tumors from other organs (Joseph, 2005). Computed Tomography (CT) is considered the most accurate modality available for early detection and diagnosis of pulmonary nodules and cancer.

Studies have been conducted [1, 4, 5, 8, 12, 13, 7, 11], automatic detection of lung nodules composed of two step, namely lung nodule candidate detection and classification to determine nodule. Detection of nodule candidates begins with lung filed segmentation. Current method is widely used for lung field segmentation of CT image is thresholding and Active Contour. Both methods are equally rely on large contrast between gray values of lung parenchyma and surrounding tissues. Research on lung segmentation, among others, study of Nomura, lung segmentation using gray-scale thresholding, component labeling,

and morphological processes. The next study is Dolejs, lung segmentation using thresholding and binary operations.

Drawbacks of both methods is that if nodule is large and located on the edge of boundary lungs, causing lung borders are not clear, so if done segmentation, nodule will not be included in lung image (part of lung that contained nodule will be lost). This means that segmentation of lung field was considered a failure, because nodules image that are focus of research will be lost. Purpose of our research is segmentation of lung field that contains abnormalities in CT scan image using registration. Registration method is used for lung segmentation is non-rigid registration methods. Non-rigid registration method consists of two activities, namely drawing lung image of defects (boundary edges damaged by large nodules), and the registration between the image that has been painted with lung image that has boundary edges abnormal.

Results of registration process is lungs image that have clear borders. Next process is the segmentation by mathematical morphology. To test accuracy of segmentation method with registration, then results will be compared with manual segmentation by groundtruth.

## METHOD

In this study we have been implementing three segmentation methods, segmentation methods based on thresholding, active contour method, and elastic registration (non-rigid registration). The third method can be described as follows:

### Segmentation with Elastic Registration

Steps of lung segmentation with an elastic registration can be shown in figure 1 below.

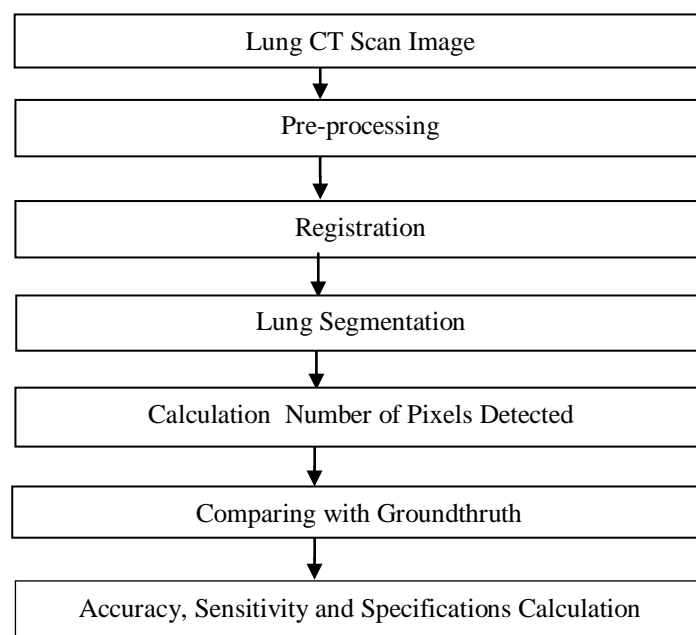


**Figure 1 Steps of Lung Segmentation System Design**

### Pre-processing

Steps in pre-processing include:

#### 1. Setting of Intensity Value

Intensity Adjustment works by performing a linear mapping of intensity values in histogram of beginning intensity values of a new histogram.

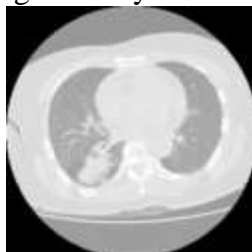


**Figure 2 Intensity Adjustment Process Results**

#### 2. Histogram Equalization

Histogram equalization is a non-linear process that aims to give a light image corresponding to human visual analysis. Histogram equalization aims to change image, so resulting image has a histogram that is more evenly, which can make all level brightness a histogram can be used. Histogram equalization is a method to improve image quality by changing distribution of gray level images (Gonzales, 1987). It is intended that a more equitable distribution of gray levels compared to original image (Tinku, 2005).



**Figure 3 Results of Histogram Equalization**

### Registration

Registration method used is non-rigid registration with Sum of Squared Differences (SSD) method. Sum of Squared Differences (SSD) is one of simplest similarity matrix. Square of difference in image intensity and intensity remains respective moving images accumulated over all voxels of image remains. Image registration are assumed identical, except for Gaussian noise. SSD can be shown by the following formula:

$$\sum_{(i,j) \in W} (I_1(i,j) - I_2(x+i, y+j))^2 \quad (1)$$

Correlation is based on the type of matching (matching) produces dense depth maps with the calculation of disparity at each pixel with the operation of neighborhood (neighborhood). This is obtained by taking the square window of certain size around the pixel is dominant in the reference image and find the pixel homologous with windows on the target image. The goal is to find correspondence (correlation) pixels with a certain disparity range  $d$  ( $d \in [0, d_{max} \dots]$ ) to minimize error and maximize the amount of similarity. The algorithm of elastic registration process can be described as follows:

1. Input to registration process is a reference image (CT image of lung abnormalities present), and image registration is a CT image containing defects and edge boundaries are drawn manually by user using matlab command `imfreehand`. Registration and a reference image can be seen in Figure 3 below.

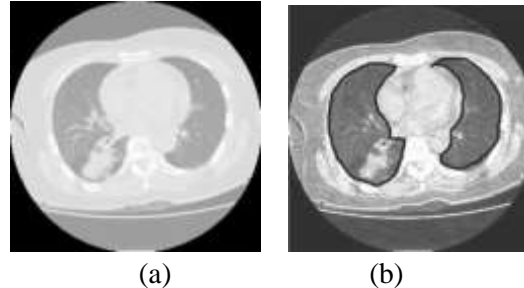


**Figure 4 Original CT image is used as reference image (a), Image Registration (Image has been Drawn Manual by User) (b)**

2. Perform non-rigid registration process from input image above, which will produce a CT image of diseased who have clear borders.

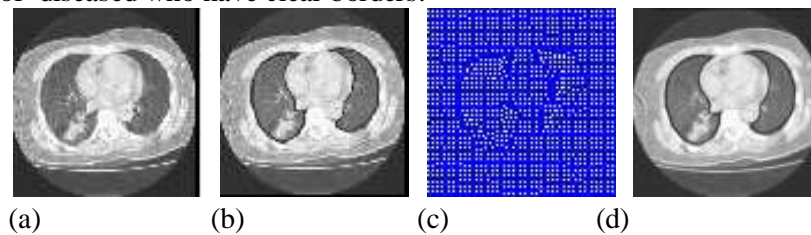


**Figure 4. Non-Rigid Registration Process**  
Reference Image (a), Registration Image (b), Registration Process (c), Image of Non Rigid Registration Result Using SSD (d)

### **Lung Segmentation**

Steps in segmentation of lung field can be explained as follows:

1. Edge Detection

Edge detection is process of detecting significant changes in gray level of an image. Changes in level of intensity is measured by a gradient image. For example, an image  $f(x, y)$  is a function of two-dimensional, then gradient vector of  $x$  and  $y$  respectively, the first derivative with respect to  $x$  and  $y$  can be written in form of equation (Mark, 2008).

$$G = \begin{bmatrix} G_x \\ G_y \end{bmatrix} = \begin{bmatrix} \frac{\partial f(x,y)}{\partial x} \\ \frac{\partial f(x,y)}{\partial y} \end{bmatrix} \tag{2}$$

Gradient operator to calculate changes in gray level intensity and direction changes. Changing are calculated by difference in value of pixel's neighbors. In two-dimensional image, gradient approximated using equation.

$$G = \begin{bmatrix} G_x \\ G_y \end{bmatrix} = \begin{bmatrix} f(x+1,y) - f(x,y) \\ f(x,y+1) - f(x,y) \end{bmatrix} \tag{3}$$

In the above equation can be written in matrix form

$$G_x = [-1 \ 1] \tag{4}$$

And

$$G_y = \begin{bmatrix} 1 \\ -1 \end{bmatrix} \quad (5)$$

While magnitude of gradient can be calculated using multiple equation models, one of equations are:

$$G[f(x, y)] = \sqrt{G_x^2 + G_y^2} \quad (6)$$

Edge detection is used in this study are: edge detection with convolution prewit method. Prewit measure used is 3x3 with horizontal elements of middle to  $G_x$  is equal to 0 and vertical elements in the middle for  $G_y$  is also equal to 0, as shown in equation 7 below.

$$G_x = \begin{bmatrix} 1 & 1 & 1 \\ 0 & 0 & 0 \\ -1 & -1 & -1 \end{bmatrix} \quad (7)$$

And

$$G_y = \begin{bmatrix} -1 & 0 & 1 \\ -1 & 0 & 1 \\ -1 & 0 & 1 \end{bmatrix} \quad (8)$$

## 2. Threshold

Thresholding is a process of separation of pixels based on degree of gray. Gray pixels that have degrees less than specified limit will be given a value of 0, while gray pixels that have a greater degree than limit value will be converted into one.

## 3. Dilation

Dilatation function is adding pixels on each edge of a binary object that is an area that has a value of 1. Where dilatation of adding 8 pixels which are interconnected to surrounding objects. And dilation is a process of incorporation of background points (0) become part of object (1). Using of dilation is to place pivot point S at point A. Give the number 1 for all points (x, y) are exposed to or affected by the structure of S at that position. Dilation equation shown in equation 9 below:

$$D(A, S) = A + S \quad (9)$$

## 4. Filling Image Areas

To fill the image area used an algorithm based on morphological reconstruction. Image area is an area of dark pixels surrounded by lighter pixels. If location of the image is determined, the next operation is to fill location using the 4-connected background neighbors for image input 2-D and 6-connected background neighbors for 3-D input. The output of this process is the area surrounded by a light-colored pixels will have value one.

## 5. Erosion

Erosion function is to remove 8 pixels of binary object associated with edges of object. Erosion is removal of object point (1) as part of background (0). Proccese of erosion is put pivot point S at point A. If any part of S which are beyond pivot point A, then removed or used as background. Erosion are shown by equation 10 below.

$$E(A, S) = A \times S \quad (10)$$

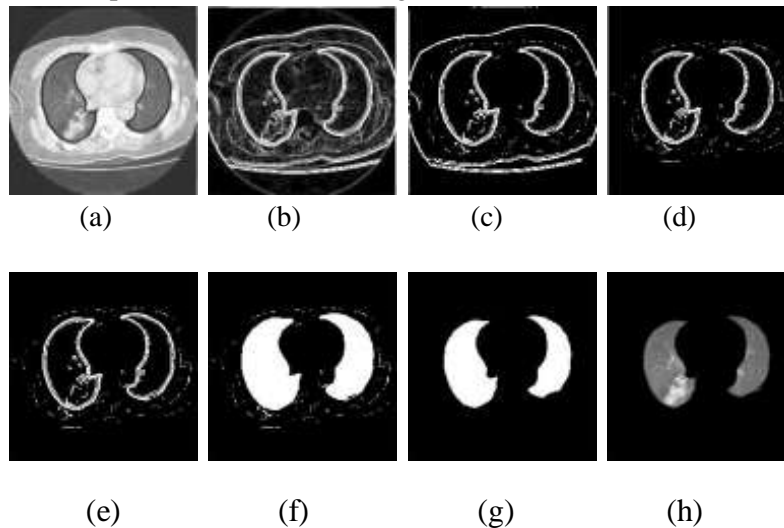
## 6. Multiplication

Image of multiplication performed to obtain final image of lung. Final lung is defined as a lung image that separated from surrounding tissue. Multiplication of image can be done by multiplying each pixel with a certain value. Can be modeled mathematically using the equation 11 below.

$$\forall f(x, y); Nf(x, y) = f(x, y) * Th \quad (11)$$

$$\forall Nf(x,y); \text{if } Nf(x,y) > 255 \text{ then } Nf(x,y) = 255 \quad (12)$$

With  $Th \geq 1$ ,  $F(x, y)$  is the original image,  $Nf(x, y)$  is Result of multiplication between original image intensity with value of  $Th$ . In our study process of multiplication is multiplication of lung mask image segmentation results with lung CT images was done histogram equalization process. Results of lung field segmentation process can be seen in figure 6 below:



**Figure 5 Result of registration (a), Image of Edge Detection Results With Convolution Prewitt (b), Image of Threshold With Threshold Value 155 (c), Image of Erosion Process Results (d), image of dilation process results By Rating: 1.5 (e), Image of Mask Process Results (f), Image of Segmentation Results (g), Finally Lung Image (results of multiplication between Image a With Image g (h)).**

#### *Calculate Pixels That Are Detected*

Image from segmentation result converted into a binary image and calculated number of pixels that are detected by displaying histogram.

#### *Comparing with Groundtruth*

Lung field segmentation process by groundtruth done by marking borders of lung on original CT image using Paint program. Image of marking of Groundtruth converted into a binary image and calculated number of pixels that are detected by displaying histogram. In this study groundtruth is a radiologist from Bethesda Hospital Yogyakarta.

#### *Calculate of Accuracy, Sensitivity and Specificity*

To calculate accuracy, sensitivity and specificity of lung field segmentation is done by adding image segmentation results using registration with ground truth segmentation results are converted into data types unsigned integer (uint8). Furthermore detected pixels are grouped into 4 groups: TP (true positive), TN (true negative), FP (false positive) and FN (false negative). TP is a lung pixel detected correctly. TN is lung pixels identified incorrectly. FP is not lung pixels

were identified as lung pixels. While FN is not detectable lung pixels. Then to test performance of proposed segmentation method by calculating accuracy, sensitivity and specificity. Accuracy indicates performance of proposed method. Sensitivity indicates lung pixels are detected correctly. Equation of accuracy, sensitivity and specificity shown in equation 7, 8, 9 below:

$$Accuracy = \frac{TP+TN}{TP+FP+FN+TN} \quad (7)$$

$$Sensitivity = \frac{TP}{TP+FN} \quad (8)$$

$$Specificity = \frac{TN}{TN+FP} \quad (9)$$

### Segmentation Using Thresholding

Steps of system design for lung segmentation with thresholding similar to steps in segmentation of lung image using registration method. That distinguish between is, in the process of segmentation by thresholding there is no registration process.

### Segmentation Using Active Contour

Steps of segmentation with active contour can be described as follows:

- a. Perform early initialization of active contour

$$C = \{(x, y) : \varphi(x, y) = 0\} \forall (x, y) \in \Omega \quad (10)$$

- b. Calculating value of u and v, which represents interior and exterior region

$$u = \frac{\int_{\Omega} I(x, y) H(\varphi(x, y)) dx dy}{\int_{\Omega} H(\varphi(x, y)) dx dy} \quad (11)$$

- c. Calculate energy of contour function

$$FF = (I-v)^2 - \lambda_2 (I-u)^2 \quad (12)$$

- d. Calculate flow

$$\frac{\partial \varphi}{\partial t} = \frac{FF}{|FF|} + \mu \cdot Curvature(\varphi) \quad (13)$$

- e. An update to its contour

$$\varphi^{t+1} = \varphi^t + \Delta t \cdot flow \quad (14)$$

- f. Process of step a, b, c, d to convergent conditions

## EXPERIMENT AND RESULTS

Dataset used is image of lung CT scans of 20 patients. Imaging performed used Thosiba TCT 300s, one of facilities owned by Bethesda Hospital Yogyakarta. Orientation of axial slices with a slice of patient is taken, so number slices are used role in the experiment amounted to 20 slices. Image size of 505x427 pixels, and thickness of 0.5 - 10 mm. Example CT image of normal and abnormal lungs with axial slices shown in Figure 8.

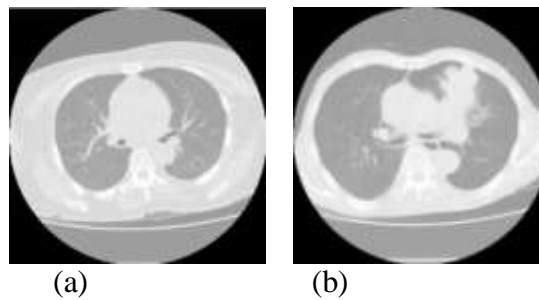


**Figure 6 Examples of CT images Lung With Axial slices Image Normal Ct Scan Lung (a), Abnormally Lung CT Scan Image (b)**

The first experiment is segmentation of lung CT image slice number 19 with big abnormality (beyond lung). Results of this experiment shows that thresholding method, image of nodules (disease) is not in image of lung. This indicates a failure of segmentation with the method. More results as shown in Figure 9 following:

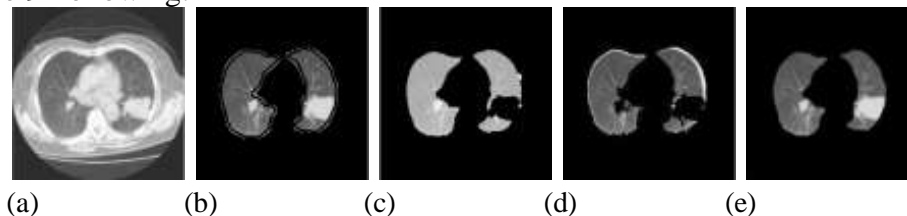


**Figure 7 Segmentation results of CT Pulmonary with Great Shape Nodules. Original Ct Image (a), Manual Segmentation Results (b), Thresholding Segmentation Results (c), Active Contour Segmentation (d), Segmentation Results With Non-Rigid Registration (e).**

Results of three segmentation methods are used can be seen that segmentation with registration have a higher accuracy compared with thresholding and active contour method. The results of the calculation accuracy of the methods used are listed in Table 2.

**Table 1 Calculation Results of Accuracy With Large Abnormalities Forms**

| Segmentation Methods | Accuracy % | Sensitivity % | Specificity % |
|----------------------|------------|---------------|---------------|
| Threshold            | 94.2       | 95.1          | 93.9          |
| Active Contour       | 92.45      | 92.49         | 92.44         |
| Registration         | 95.4       | 90.8          | 97            |

To clarify performance of method used, we also performed reconstruction of three-dimensional (3-D) image of segmentation with registration. 3-D reconstructions can be shown in following figure.

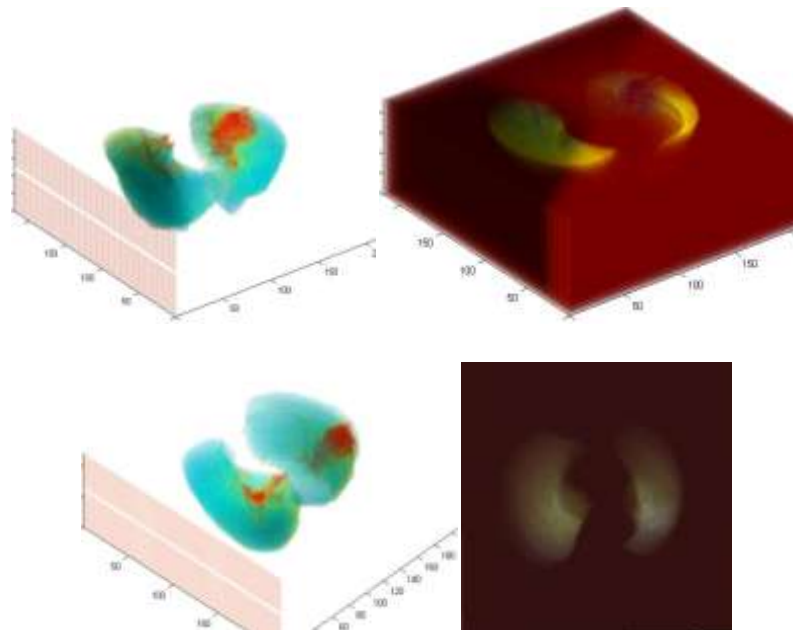


**Figure 8 Results of 3-D Visualization**

The next experiment is segmentation of one slice normal lung CT image. Results of this experiment shows that for normal lung, thresholding method has a higher accuracy rate than registration method. More results as shown in Figure 11 below:

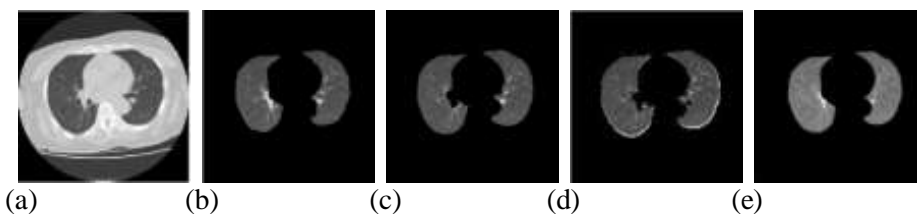


**Figure 9 Segmentation Results of the Normal Lung**  
**Original Ct image (a), Manual Segmentation (b), Thresholding Segmentation (c), Active Contour Segmentation (d), Segmentation Results With Non-Rigid Registration (e).**

**Table 2 Accuracy of the Normal Lung Segmentation**

| Segmentation Methods | Accuracy % | Sensitivity % | Specificity % |
|----------------------|------------|---------------|---------------|
| Threshold            | 93.3       | 88.3          | 94.5          |
| Active Contour       | 94.9       | 88            | 96.9          |
| Registration         | 95.1       | 92.8          | 95.6          |

3-D reconstructions of normal lung can be shown in the following figure.

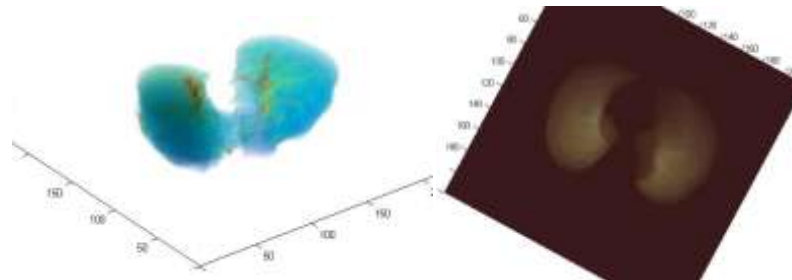


**Figure 10 Visualization of 3-D Image of Normal Lung**

Experimental results using 20 slice CT scans of patients can be seen that registration method has higher accuracy than other two methods, namely the threshold and the active contour. This shows registration segmentation method is suitable to segments lung with containing abnormalities. Result of comparison of three methods used are listed in Table 4.

**Table 3 Segmentation results Using Three Methods With All Data**

| Data | Segmentation Methods  | Accuracy % | Sensitivity % | Specificity % |
|------|-----------------------|------------|---------------|---------------|
| All  | Threshold             | 92.2       | 91.3          | 92.4          |
|      | <i>Active Contour</i> | 92.4       | 87.5          | 93.7          |
|      | Registration          | 95.5       | 91.5          | 96.6          |

## CONCLUSION

Conclusion from above experiments is that segmentation by thresholding and active contour methods fail to segment pulmonary CT images containing disease (abnormalities). This is due in pulmonary with large nodules size have lung borders are not clear (low contrast value). Segmentation by registration can be identified region of lung CT with large abnormalities form. Segmentation by thresholding and active contour can run well on lung CT scan image that have small diseases shape or in lung that had no disease (normal lung).

## DISCUSSION

Our research successfully segmenting diseased lung (abnormal), which can not be done by conventional methods, but process still requires intervention of user (process of manually drawing in abnormal lung CT image. Therefore, this method can be improved towards automation, so user intervention can be reduced. For further research we tried to use a segmentation method with supervise, for consideration method is to use Active Shape Model (ASM).

**REFERENCES**

- [1] D. Cascio, S. C. Cheran, A. Chincarini, G. De Nunzio, Automated Detection of Lung Nodules in Low-dos Computed Tomography, International Journal of Computer assisted Radiology and Surgery, Vol 2, Supplement 1, June 2007.
- [2] Gonzales, R. C., Woods, R. E. And Eddins, S., Digital Image Processing Using Matlab, 1st Edn, Printice Hall, 2003.
- [3] Hohne, K. H., M. Bomans, et al. (1990). "Rendering Tomographic Volume Data: Adequacy of Methods for Different Modalities and Organs." 3-D Imaging in Medicine F60: 197-215.
- [4] Heidi C Roberts, Anna Walsham, Errol Colak, Hany Kashani, Chris Mongiardi, Demetris Patsios, The Utility of Computer-aided-detection for the Assessment of Pulmonary Arterial Filling detects at CT Angiography, University Healt Network, Toronto, ON, Canada, International Journal of Computer assisted Radiology and Surgery, Vol 2, Supplement 1, June 2007.
- [5] Ilaria Gori, A Multi-Scale Approach to Lung Nodule detection in Computed Tomography, Istituto Nazionale di Fisica Nucleare, Sezione di Pisa Italy, International Journal of Computer assisted Radiology and Surgery, Vol 2, Supplement 1, June 2007.
- [6] Jusuf A, Harryanto A, Syahrudin E, Endardjo S, Mudjiantoro S, Sutandio N. Type of lung cancer non-small cell carcinoma. National guidelines for diagnosis and management in Indonesia, 2005. PDPI dan POI, Jakarta, 2005.
- [7] L. Borosky, M. C. Lee, L. Zhao, L. Agnihotri, C. A. Powell, Computer-aidec Diagnosis for Lung cancer Using a Classifier Ensemble, College of Physicians and Surgeons, New York, NY, USA, International Journal of Computer assisted Radiology and Surgery, Vol 2, Supplement 1, June 2007.
- [8] Martin Dolej s, Jan Kybic, The Lung TIME Annotated Lung Nodule Dataset and Nodule Detection Framework, Faculty of Electrical Engineering, Czech Technical University in Prague, Czech Republic.
- [9] Mark S. Nixon A and Alberto S. Aguado, (2008), "Feature Extraction And Image Processing", Second Edition, AcademicPress is an imprint of Elsevier.
- [10] M. Syamsa Ardisasmita, Image Segmentation and Reconstruction Organ In Three Dimensions Using Mathematical Morphology and triangulated, Center for Computing and Information Technology Development BATAN.
- [11] Sumiaki Matsumoto, Yoshiharu Ohno. Hitosi Yamagata, Departement of Radiology, Kobe University Graduate School of Medicine , Japan, International Journal of Computer assisted Radiology and Surgery, Vol 2, Supplement 1, June 2007.

- [12] Takeshi Hara, Xiangrong Zhou, Shoji Okura, Hiroshi Fujita, Takuji Kiryu, Hiroaki hoshi, Nodule Detection Methods Using autocorrelation Feature on 3D chest CT Scans, Departement of Intelligent.
- [13] T.Kobota, A. Jerebko, M. Salganicoff, A. Krishnan, A Segmentation Algorithm With Competition-diffusion and Distance Transform For Automated Estimated of Pulmonary Nodule Diameter, Susquehanna University, Mathematical Sciences, Selinrove PA USA, International Journal of Computer assisted Radiology and Surgery, Vol 2, Supplement 1, June 2007.
- [14] Tinku Acharya and Ajoy K., (2005), "Ray Image Processing Principles And Applications", A John Wiley & Sons, Mc., Publication.